Pis'ma v ZhETF, vol. 84, iss. 9, pp. 584 – 589

Interference effects in the emission spectra of QD's in high quality cavities

L. V. Keldysh[+*], *V. D. Kulakovskii*[*∇], *S. Reitzenstein*[*], *M. N. Makhonin*[*∇], *A. Forchel*[*]

[+] *Lebedev Physical Institute RAS, Moscow, Russia*

[*] *Technische Physik, Wuerzburg University, Wuerzburg, Germany*

[∇] *Institute of Solid State Physics, RAS, 142432 Chernogolovka, Russia*

Submitted 3 October 2006

We have investigated theoretically and experimentally the emission of QD-cavity systems for different coupling strength and a wide range of exciton-photon mode detunings controlled by temperature variation in the range of 10–45 K. Under close to resonance conditions the radiation spectrum from the cavity emission becomes essentially dependent on the primary excitation path, which can be either via resonant QD exciton or via cavity mode. Particularly, in the case of nonresonant cavity mode excitation the emission line becomes split in two asymmetric lines already in the weak coupling regime.

PACS:

Since its proposal by Purcell [1] and work involving atoms in cavities (see, for example, [2]), cavity quantum electrodynamics (CQED) has been actively pursued for its potential to investigate fundamental problems in light matter interaction. Light confinement in the cavities modifies both, modes of photon states, to which the electronic transitions of atoms can couple, and coupled light matter states. A central aspect of cavity research over the years has been the modification of spontaneous emission rates [1, 3] in the regime of weak coupling between the electronic and photonic excitations, which opens opportunities for basic physics studies as well as in semiconductor optoelectronics, in particular, for light emitting diodes and quantum computing or quantum cryptography. One major current trend addresses the achievement of strong coupling between confined electronic and photonic states of low dimensionality. These systems are characterized by an exciton – photon interaction rate which is faster than the rate of any dissipative channel. In this situation coupled modes come to existence, which are superposition of photon and electronic excitation [4, 5].

Semiconductor quantum dots (QDs) that exhibit a discrete density of electronic states can be used in semiconductor cavities as quasi-atomic light emitters. Semiconductor optical microcavities (MC) providing strong photonic confinement in one direction have been fabricated from high quality layered semiconductors more than 10 years ago [6]. Recently, solid state CQED using QDs in semiconductor MCs with three dimensional optical confinement has become a central research field [7, 8]. The simplest semiconductor system representing the "ultimate" case with both electrons and photons confined in all dimensions is a 3D confined pillar MC with a single QD in the active layer. Such a system should exhibit peculiar effects characteristic of a two-level atom in interaction with an optical cavity, e.g. an enhancement or inhibition of the spontaneous emission rate in the weak coupling regime (Purcell effect) and vacuum-field Rabi splitting in the strong coupling regime. In semiconductor MCs, the optical modes, C, are coupled to electron-hole excitations in the QD, X, forming coupled exciton-photon states. The splitting and the decay of these modes provide important insight into their couplings to the environment, and they also play a critical role in applications of the optical systems.

In the treatment of coupled modes, the electronic excitations, which are electron-hole pairs or excitons in the case of semiconductors, are usually represented by either two-level systems or by harmonic oscillators [9, 10]. Within these coupled mode treatments in a simple approximation, phenomenological broadening parameters often are used to represent the linewidths of the electronic transition and also the finite quality factor Q of the cavity [11]. Of course, such a representation of the damping is physically less realistic for the photon as its linewidth arises from coupling to the continuum of delocalized photon modes outside the cavity rather than from a true dissipative mechanism. However a more detailed consideration of effects of dissipation and mode broadening in the emission spectra of optical cavities with the use of Fano type models [12] has shown that the simple approximation describes the main features of the emission spectra [13].

In the simple approximation, for energy levels of interacting QD exciton (X) and cavity (C) modes at a resonance ($E_X = E_C = E_0$) the energies of interacting modes are

$$E_{1,2} = E_0 - i(\gamma_C + \gamma_X)/2 \mp \{g^2 - (\gamma_C - \gamma_X)^2/4\}^{1/2} \quad (1)$$

where $2\gamma_{C,X}$ is the FWHM of the cavity (exciton) mode, $2\gamma_C = E_C/Q \gg \gamma_X$, and g is the "vacuum Rabi splitting" parameter, equal to the scalar product of the transition matrix element of the QD dipole moment with the local value of the electric field at the dot position in a cavity containing one photon [14]. The criterion for the strong coupling regime of the QD exciton and MC modes can be approximated as $g > \gamma_C/2$ and the strong coupling regime is fixed as an anticrossing of coupled QD exciton and cavity modes. Indeed, it follows from Eq.(1) that in the opposite, $g < \gamma_C/2$, case, referred to as a weak coupling regime, the interaction on resonance of exciton and cavity mode results in an enhanced or decreased radiative decay of QD excitons.

A simplified analysis of emission spectra based on Eq.(1) uses a lineshape fit with two Lorenzians. However, such an approximation does not take into account interference effects that can result in a strong modification of the emission spectrum. The influence of the interference effect on the emission spectra is one of the main goals of this paper. We have investigated photoluminescence of MCs based on a one λ GaAs cavity sandwiched between high reflectance GaAs/AlAs Bragg mirrors. The Bragg reflectors are composed of 20 to 26 (23 to 30) periods of $\lambda/4$ GaAs/AlAs (69 nm/82 nm) layers in the top (bottom) mirrors. The GaAs cavities (thickness one λ) contain random ensembles of $In_xGa_{1-x}As$ QDs placed at the antinode of the on-axis resonant fundamental mode of the planar cavity. The quality factor $Q = \lambda_C/\Delta\lambda_C$ of the planar resonators is in the range of several 10.000. All structures are grown by solid source molecular beam epitaxy. High-Q cavities with small mode volumes have been fabricated from these epitaxial samples. Micropillars with circular cross-sections (diameters from 1.5 to 4 μm) have been processed by electron-beam lithography and reactive ion-etching in inductively coupled or electron cyclotron enhanced Ar/Cl_2 plasmas. The strong lateral mode confinement in the micropillars is obtained by total internal reflection at the pillar sidewalls. By using an optimized deep etching processes through almost the total height of the MCs (5 μm) very smooth pillar side walls are obtained [31]. The combination of a high-Q epitaxial cavity with optimized micropillar processing allows us to realize micropillars with Q factors above 5.000 down to 1.5 μm diameter.

In our samples the cavity mode is located at the low energy side of the QD emission band, where the QD energies are well separated. The energy of single QDs is tuned on resonance with the cavity mode by using the temperature dependent shift of the band gap in the dots. PL of single pillars has been measured using a microPL setup based on a spectrometer and a nitrogen cooled CCD-camera with a spectral resolution of 0.04 meV. A microscope objective has been used to focus the laser beam into ~ 3 μm diameter spot at the pillar and to collect the pillar emission. The excitation was carried out by an Ar-ion laser ($\lambda = 514$ nm).

Fig.1a shows set of spectra recorded for a MC with a diameter of 1.8 μm and self assembled $In_{0.6}Ga_{0.4}As$

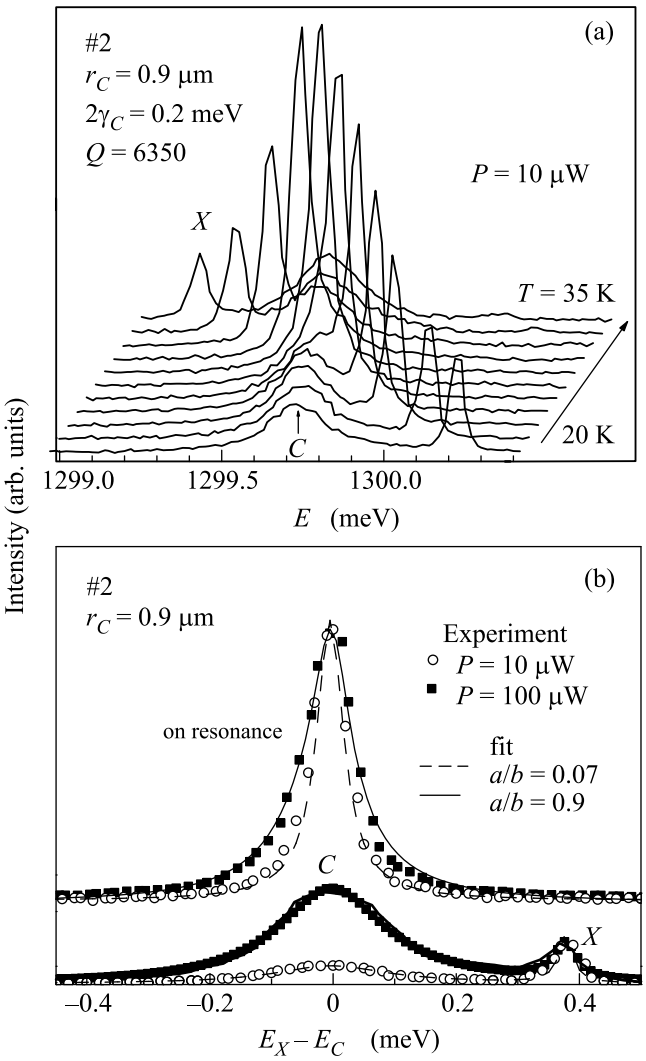

Fig.1. (a) Set of PL spectra recorded for the pillar (#2) with weak exciton-photon coupling in the temperature range of 20–35 K. (b) Comparison of PL spectra at two excitation densities, points – experiment, Lines – calculations

QDs as active material in the temperature range of 20–35 K. The spectrum at the lowest temperature consists of a narrow line corresponding to the exciton emission of single QD with FWHM $2\gamma_X$ within 0.055 meV and a markedly thicker line C ($2\gamma_C = 0.2$ meV) corresponding to the cavity mode with $Q = 6350$. The variation of the temperature allows one to tune the QD emission on and off the resonance with cavity mode. The most pronounced effect observed when tuning the QD through the cavity mode is a strong increase in the QD emission intensity. The cavity emission is nearly independent of the $X-C$ mode detuning $\Delta = |E_X - E_C|$ at $\Delta > 0.2$ meV.

Fig.2 displays spectra from a MC with a diameter of 1.6 μm and a much higher finesse $Q = 12000$ (pillar #5). At 20 K the emission of this pillar consists of the cavity mode centered at about 1.3273 eV and a QD exciton emission at slightly higher energy (1.3278 eV). For increasing temperature the pillar emission consists of two distinct lines in the whole range of temperatures, however, at 35 K the components of the emission have exchanged their properties. Over the entire temperature range the energies of the two contributions to the spectrum are well separated and avoid crossing each other, which indicates the strong coupling between the single QD exciton and cavity-mode. During the transformation of the X into the cavity mode its FWHM increases monotonically from ~ 0.05 meV to 0.11 meV whereas the FWHM of the cavity line decreases during its transformation into the X mode from 0.11 meV to ~ 0.05 meV. Finally, note as well, that the relative emission intensity of X-like and C-like modes from the pillar with strong exciton-photon coupling – similar to that from the cavity with weak coupling (Fig.1a) depends on the $X-C$ detuning, however, the intensity of the cavity-like mode is rather strong both with and without a dot on resonance.

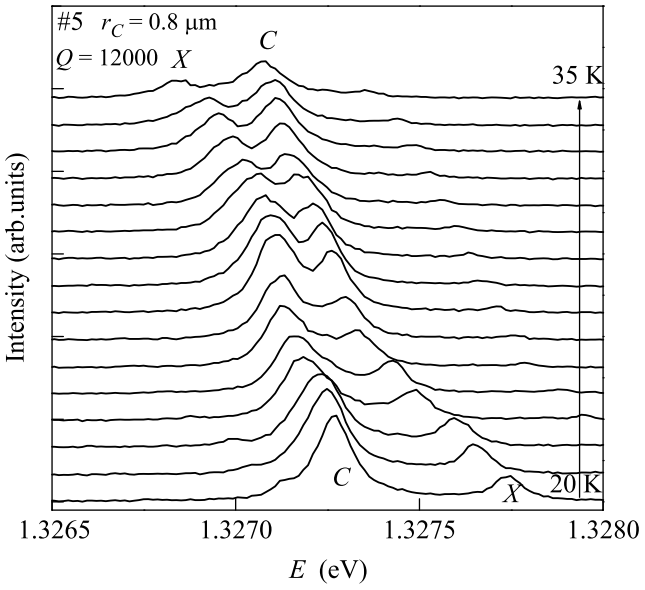

Fig.2. Set of PL spectra recorded for the pillar (#5) with strong exciton-photon coupling in the temperature range of 20–35 K

For above band gap excitation as used in the experiment, an expected main excitation channel of the $X-C$ system is the capture of photoexcited excitons by the QD with following relaxation to the lowest QD state. This channel supposes a very weak excitation of the cavity mode far from $X-C$ resonance. The observed rather strong cavity emission even out of $X-C$ mode resonance indicates an independent excitation of the cavity mode. This excitation can take place via an inelastic (e.g. phonon assisted) recombination of bulk and non-resonant QD excitons. The relative contribution of this channel is expected to increase strongly with excitation density when the capture of excitons by the QD is saturated due to a finite lifetime of the QD exciton. Such increase is well seen in Fig.1b displaying spectra for the MC #2 recorded at two different excitations. At large $X-C$ detuning, the relative intensity of the cavity emission increases more than 3 times when P increases from 10 to 100 mW. On resonance the main effect of increased excitation density is a strong line broadening. Thus, both excitation channels should be taken into account for the correct description of the emission spectra.

In a simple approximation, phenomenological broadening parameters can be used to represent the linewidths of the electronic transition and the cavity mode. In this approximation the spectral density of the electromagnetic radiation from the cavity with a set of QDs in the active layer is

$$I_c(\omega) = 2\omega\gamma_c \cdot \frac{\Lambda_c}{[\omega - \Omega_c - P(\omega)]^2 + [\gamma_c + Q(\omega)]^2} \quad (2)$$

if the primary incoherent excitation comes into the cavity mode, and

$$I_x(\omega) = \sum_j \big((2\omega\gamma_c \cdot |g_j|^2\Lambda_j)/([(\omega - \Omega_c - P(\omega))(\omega - \Omega_j) - (\gamma_c + Q(\omega))\gamma_j]^2 + [\gamma_c(\omega - \Omega_c - P(\omega)) + [\gamma_c + Q(\omega))(\omega - \Omega_j)]^2\big) \quad (3)$$

if the primary excitation comes through the resonant QD.

In these formulae ω is the photon energy, index j denotes the j-th QD, Ω_j and Ω_c are corresponding resonant photon energies, γ_j and γ_c are the linewidths, Λ_j

and Λ_c are the incoherent excitation rates. $P(\omega)$ and $-Q(\omega)$ are real and imaginary parts of the polarizability of the whole ensemble of QDs

$$P(\omega) - iQ(\omega) = \sum_j \frac{|g_j|^2}{\omega - \Omega_j + i\gamma_j}, \qquad (4)$$

g_j is the "vacuum Rabi splitting" for j-th QD.

Note here that for the case of a single QD in exact resonance with the cavity mode the definition of $I_C(\omega)$ and $I_X(\omega)$ practically coincides with formulae (37) and (36) in [13] calculated taking into account the effects of (i) the interaction of the electromagnetic mode with a continuum of electromagnetic modes within a Fano model and (ii) the coupling of the electronic excitations to a dissipative source in the QD.

Both functions $I_C(\omega)$ and $I_X(\omega)$ describe the radiation in the cavity mode, hybridized with QD resonances. However, they refer to two different mechanisms (channels) of the primary excitation discussed above. The distinction considers which of the hybridization partners – cavity mode or quantum dot excitation – is pumped directly by the primary excitation. The function $I_X(\omega)$ corresponds to the process of a primary excitation of QDs (photoexcited exciton is trapped by the QD, then being relaxed to the lowest QD state, which is resonant and therefore hybridized with the cavity mode). The hybridization itself corresponds to the partial transfer of the excitation into the electromagnetic field. Unlike that the function $I_C(\omega)$ refers to a process where the primary excitation occurs in the cavity mode, and then becomes hybridized. As indicated above, this channel may be due to inelastic (e.g. phonon assisted) recombination of bulk excitons, or a similar process with excitons trapped by nonresonant QDs, etc. In a mechanical analogy one can think about pushing either one or another of two coupled nonidentical oscillators, while always observing the response of the one of them corresponding to the electromagnetic field. Surely, in any case both degrees of freedom become excited, however, with amplitude and phase relations essentially depending on the excitation path.

The mathematical manifestation of that is clearly seen in the analytical structure of the spectral functions. Both $I_C(\omega)$ and $I_X(\omega)$ have exactly the same set of poles – hybridized mode frequencies – in the complex plane. However, the shape of the spectra may differ drastically due to the difference in residue values. Even in the simplest case of a single resonant QD the plots of $I_C(\omega)$ and $I_X(\omega)$ look like mutually complementary. This is shown in Fig.3. The difference is strongest at small exciton-photon coupling $g \sim \gamma_X \ll \gamma_C$ when the transfer of excitation from QD to cavity mode as well as that from cavity to QD is relatively weak. In this case the primary excitation of the QD results in a very narrow line with FWHM $2\gamma \sim 2\gamma_X$. In contrast, the excitation of the cavity mode results in a wide line (FWHM $2\gamma \sim 2\gamma_C$) with a relatively weak narrow dip at the QD exciton frequency. The qualitative difference in the spectra continues till the strong coupling regime realizing at $g > \gamma_C/2$ and providing the strong enough exchange between the cavity and QD modes. In particular, Fig.3 shows that even at $g \sim 3/4\gamma_C$ a marked splitting in the spectrum is observed only for a primary excitation of the cavity mode. With increasing g the qualitative difference between $I_C(\omega)$ and $I_X(\omega)$ disappears, however the quantitative difference is well pronounced even at $g \sim 2\gamma_C$.

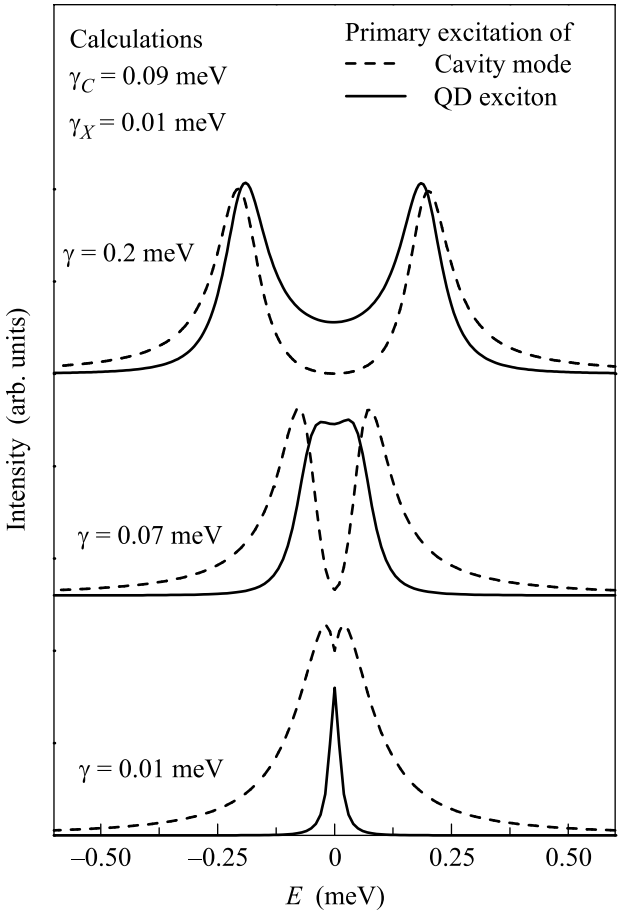

Fig.3. Plots of $I_C(\omega)$ (dot lines) and $I_X(\omega)$ (solid lines) calculated for the on resonance condition at $g = \gamma_X \ll \gamma_C$ (lower panel), $\gamma_X \ll g \sim 3/4\gamma_C$ (middle panel), and $\gamma_X \ll \gamma_C < g$ (upper panel)

A detailed comparison of PL spectra for the two excitation mechanisms and various $X-C$ mode detunings near the transition from the weak to the strong coupling regime is presented in Fig.4. For the parameter range

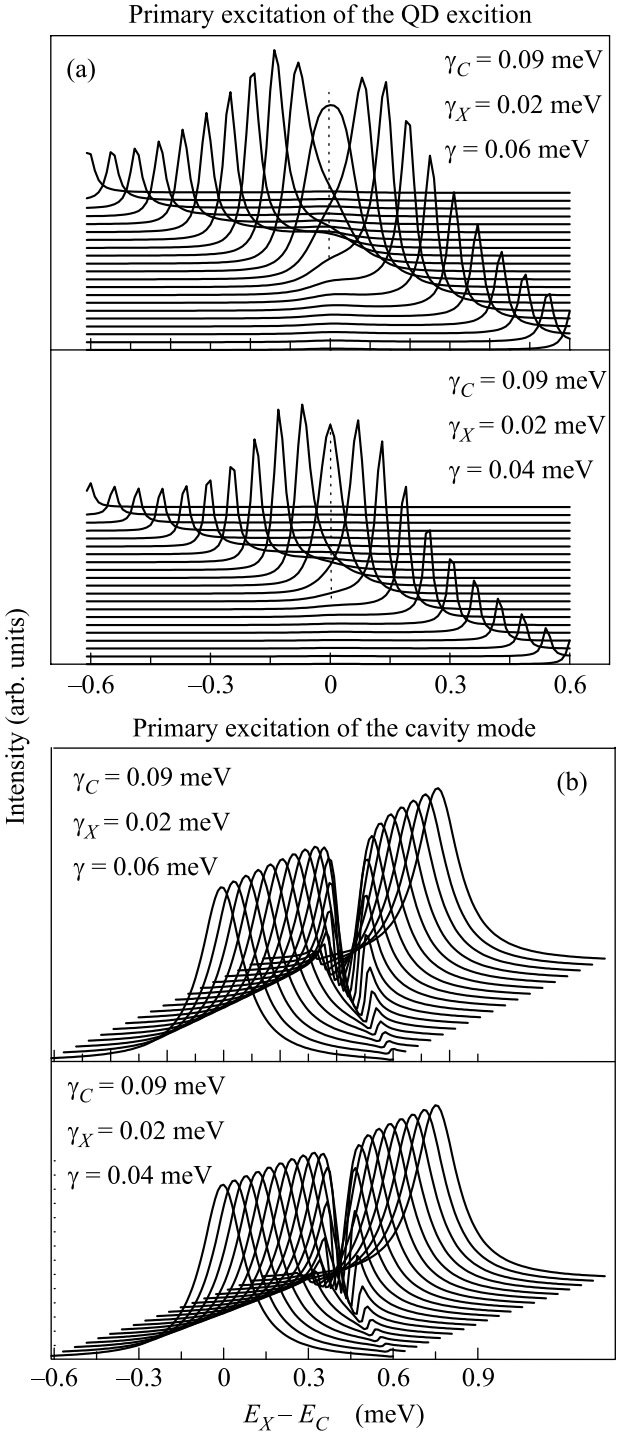

Fig.4. Comparison of PL spectra for various $X-C$ mode detuning and g/γ_X, g/γ_C ratios for two excitation mechanisms: primary excitation of the cavity mode (left panel) and QD exciton (right panel)

$\gamma_X < g < \gamma_C$, the dominating feature in the $I_X(\omega)$ plot is a steep increase of a narrow peak of the dot emission in the frequency range few γ_C wide around the cavity mode. The cavity mode itself is practically invisible until some dot approaches the resonance. Unlike that the $I_C(\omega)$ plot is dominated by the strong and relatively broad cavity emission line, cut, however, by a narrow dip – a precursor of the Rabi splitting – at the resonant QD frequency. The intensity of the cavity emission is nearly independent of the $C-X$ detuning. The dip in the spectrum results from the mode interference and exists for $|g|^2 > \gamma_X^3/(2\gamma_C)$, i.e. long before two coupled modes become resolved. The FWHM of the dip is equal to $\sqrt[4]{|g|^4 + 2\gamma_C\gamma_X \cdot |g|^2}$, i.e. at weak coupling regime exceeds essentially the Rabi splitting. In contrast, the dip in the $I_X(\omega)$ plot appears only when the usual strong coupling condition $|g|^2 > \frac{1}{2}(\gamma_C^2 + \gamma_X^2)$ is fulfilled.

As was mentioned before, under above band excitation both channels of excitation via the QD and the cavity modes should be taken into account. In this case the PL spectrum at low excitation density is given by

$$I(\omega) = I_c(\omega) + I_{dot}(\omega), \quad \Lambda_c = a\Lambda, \quad \Lambda_{dot} = b\Lambda, \qquad (5)$$

where a and b are the partial excitation rates in corresponding channels. In the weak and the beginning of the strong coupling regimes the peaks of the second term overlap the dip of the first one, which makes the plot more complicated and demands a more detailed analysis to extract the exciton-photon coupling constant in the MC.

Figure 5 shows the simulation of emission spectra for two MCs with the use of formulas (2)–(5). The ratio a/b is determined from the fit of the whole set of pillar spectra recorded for various $X-C$ detuning. The spectra for the 1.8 μm pillar (#2) with a weakly coupled QD exciton and cavity modes shown in Fig.1a are well reproduced with the use of the ratio $a/b = 0.07$. The main effect of a relatively weak direct excitation of the cavity mode is a well pronounced cavity emission at large Δ. The QD emission intensity increases strongly at the resonance with the cavity mode, whereas its halfwidth changes relatively weakly, as expected for the system far from the strong coupling regime ($g = 0.3$ is nearly twice smaller than the critical value $g > 0.5$ meV for this MC). As was discussed above in Fig.1b, an increase of excitation power leads to an increasing contribution from the primary excitation via cavity channel and leads to a strong line broadening at zero detuning. The solid and dashed curves in Fig.1b show the fit of the spectra recorded at low and high excitation densities, respectively, with the same values of exciton and cavity decays but different ratios of cavity to QD channel contributions.

Figure 5b shows the simulation of the spectra from pillar #5 demonstrating a well pronounced anticrossing behavior with the use of Eqs.(2)–(5). Comparison of

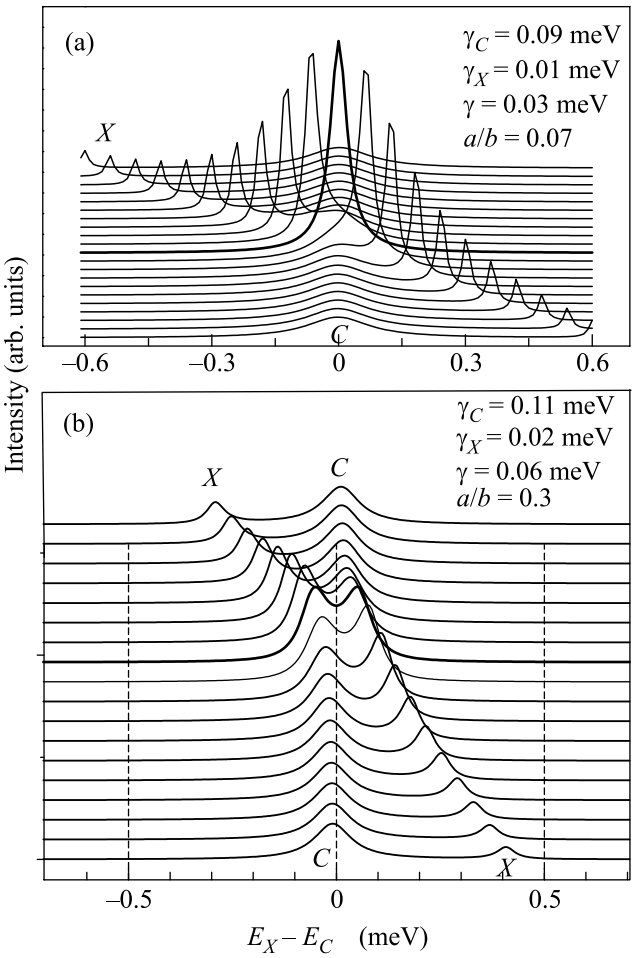

Fig.5. PL spectra calculated for the pillars with a weakly (#2) and strongly (#5) coupled QD exciton and cavity modes

Figs.2 and 5b shows, that the experimental spectra are qualitatively well reproduced by taking the ratio of the primary excitation of the cavity mode to that of the QDs $a/b = 0.3$. The best fit of the set of spectra is obtained using a coupling constant $g = 0.06 + / - 0.004$ meV. This value is twice as much as that required for weak-to-strong coupling transition, $g = 0.03$ meV. Note that in a simplified two-oscillator model the value of g is equal to one half of line splitting in the emission spectra recorded at zero detuning. For pillar #5 demonstrating a splitting of $\Delta = 0.14$ meV this results in a value of $g = 0.07$ meV, that exceeds the value of g extracted with account for different excitation channels by more than 10%. This indicates the importance of the correct account for both cavity and QD primary excitations even in the strong coupling regime.

In conclusion, by comparing measured PL spectra with theory we have shown that the MC pillar spectra depend strongly on the primary excitation mechanism via QD excitons or the cavity mode. In the case of primary QD excitation the PL spectra demonstrate (i) extremely weak cavity emission, (ii) strong Purcell effect, and (iii) a line splitting only in the strong coupling regime. In contrast, under the excitation of the cavity mode the spectra demonstrate (i) strong cavity emission and (ii) a well pronounced dip in the cavity peak instead of Purcell enhancement. The dip appears at very weak coupling, well before the strong coupling regime, and its halfwidth exceeds strongly the exciton-photon coupling constant g.

We gratefully acknowledge the provision of high quality samples for the experiments used to compare with the model calculations by J.P. Reithmaier, A. Löffler, and M. Kamp. Financial support of RFBR, INTAS, Deutsche Forschungsgemeinschaft and the State of Bavaria is gratefully acknowledged.

1. E. M. Purcell, Phys. Rev. **69**, 681 (1946).
2. C. Weisbuch, *Cavity Quantum Electrodynamics*, Ed. P. Berman, Academic Press, San Diego, 1994.
3. R. G. Hulet, E. S. Hilfer, and D. Kleppner, Phys. Rev. Lett. **55**, 2137 (1985); D. Kleppner, Phys. Rev. Lett. **47**, 233 (1981).
4. J. P. Reithmaier, G. Sek, A. Loeffler et al., Nature **432**, 197 (2004).
5. T. Yoshie, A. Scherer, J. Hendrickson et al., Nature **432**, 200 (2004).
6. C. Weisbuch et al., Phys. Rev. Lett. **69**, 3314 (1992).
7. Y. Yamamoto and R. E. Slusher, Physics Today **46**, 66 (1993).
8. J. M. Gerard and B. Gayral, Physica E **9**, 131 (2001); K. J. Vahala, Nature **424**, 839 (2003).
9. V. Savona, Z. Hradill, A. Quattropani et al., Phys. Rev. B **49**, 8774 (1994).
10. L. C. Andreani, V. Savona, P. Schwendimann et al., Superlattices Microstruct. **15**, 453 (1994).
11. Y. Zhu, D. J. Ganthier, S. E. Moriu et al., Phys. Rev. Lett. **64**, 2499 (1990).
12. U. Fano, Phys. Rev. **124**, 1866 (1961).
13. S. Rudin and T. L. Reinecke, Phys. Rev. A **62**, 053806 (2000).
14. L. Andreani, G. Panzarini, and J. M. Gerard, Phys. Rev. B **60**, 13276 (1999).